Thermal and X-ray Investigation on the Coexisting Smectic Mesophases of a Liquid Crystalline Side-Chain Polymer

G. Galli and E. Chiellini*

Dipartimento di Chimica e Chimica Industriale, Via Risorgimento 35, 56126 Pisa, Italy

M. Laus and A. S. Angeloni

Dipartimento di Chimica Industriale e dei Materiali, Viale Risorgimento 4, 40136 Bologna, Italy

O. Francescangeli and B. Yang

Dipartimento di Scienze dei Materiali e della Terra, Via Brecce Bianche, 60131 Ancona, Italy

Received July 9, 1993
Revised Manuscript Received October 28, 1993

In recent papers,[1,2] we discussed the synthesis and liquid crystalline properties of new specifically designed main-chain and side-chain polymers, containing prochiral sulfide moieties, suitable for modification by asymmetric oxidation yielding the corresponding chiral sulfoxide-containing polymers. The introduction of the strong dipole moment of the sulfoxide moieties, directly located at the chiral center and perpendicular to the long axis of the mesogenic groups, is expected to be a structural feature conducive to chiral smectic mesophases with potential applications in electrooptics and nonlinear optics.

Within our continuing interest in elucidating the transitional characteristics of these classes of polymers, we describe the peculiar phase behavior of the side-chain polymer sample **I-8**:

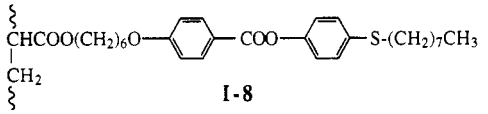

I-8

This polymer ($n = 8$) belongs to a series of homologues **I-*n*** ($n = 1$–10) where n is the number of carbon atoms in the terminal thioalkyl tail; it was prepared by free-radical polymerization of the corresponding acrylate using 2,2′-azobis(isobutyronitrile) as the initiator according to ref 2. The number-average molar mass (M_n) and the first polydispersity index (M_w/M_n) of polymer sample **I-8** as determined by SEC were 62 000 and 1.9, respectively. The thermal and liquid crystalline behavior of polymer **I-8** was studied by combined differential scanning calorimetry, optical microscopy observations, and X-ray diffraction analysis on unoriented and oriented specimens. Figure 1 shows the DSC heating and cooling curves, as recorded after annealing the sample by cooling at 10 K min^{-1} from the isotropic melt. On heating, a step due to the glass transition at 299 K and three endothermic transitions at 314, 352, and 365 K, with associated entropy changes of 2.5, 6.5, and 11.1 J mol^{-1} K^{-1}, respectively, are observed. On cooling, all the transitions are reversed with relatively low degrees of supercooling. When observed between crossed polarizers, **I-8** exhibits a faint birefringence in the glassy state. Above the glass transition, a viscous fluid with smectic fan textures exists up to the isotropization point. No unambiguous identification of the nature of the smectic mesophases of this polymer sample was, however, possible by optical microscopy observations. X-ray diffraction analysis better clarifies the smectic mesomorphism of **I-8**. Figure 2 illustrates the X-ray powder patterns of **I-8**, after annealing by cooling from the isotropic melt, at different temperatures from room

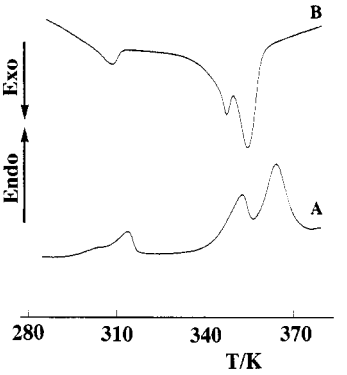

Figure 1. Second DSC heating (A) and cooling (B) curves (10 K min^{-1}) for **I-8** after first cooling from the isotropic melt.

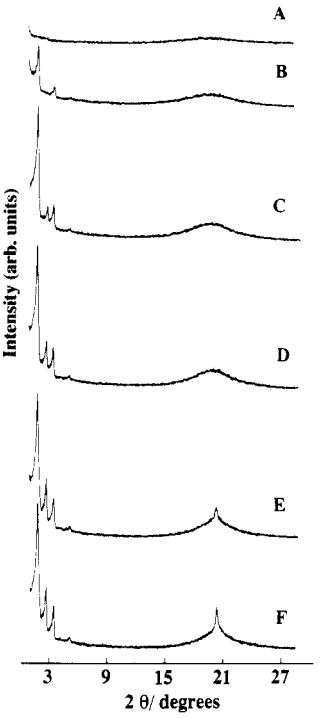

Figure 2. X-ray diffraction diagrams on the second heating cycle for **I-8** at 373 (A), 363 (B), 353 (C), 343 (D), 313 (E), and 298 K (F).

temperature up to the isotropization point. At room temperature, the X-ray diagram (Figure 2F) consists of four small-angle reflections of decreasing intensity, that correspond to periodicities (d) of 52.4, 34.6, 26.2, and 17.4 Å, and a wide-angle sharp signal at $D = 4.4$ Å. Comparing the values of the lattice spacings, it appears that the small-angle peaks at $d = 26.2$ and 17.4 Å are the first two consecutive orders of 52.4 Å, whereas no correlation exists with the periodicity of 34.6 Å. These small-angle signals suggest the presence at room temperature of layered structures with two different periodicities, namely, $d =$ 52.4 and 34.6 Å. They will be referred to as d_1 and d_2, respectively. The interlayer period d_2 is equal to the length (L) of the side chains, as evaluated from standard bond lengths and angles under the assumption of an *all-trans* conformation ($L \approx 34.5$ Å), indicating the presence of a monolayer structure, whereas the stacking period d_1 is less than twice the extended molecular length, thus implying some form of bilayer structure.

The wide-angle peak becomes very diffuse at temperatures above 315 K (compare parts E and D of Figure 2), corresponding to the temperature relevant to the first DSC endothermic transition. The broadening of the wide-angle

0024-9297/94/2227-0303$04.50/0

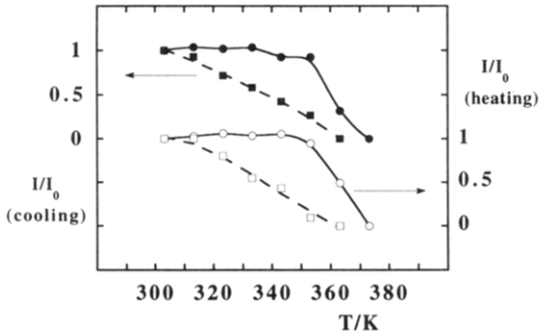

Figure 3. Trends as a function of temperature of the intensity of the first-order reflection associated to periodicities d_1 (○,●) and d_2 (□,■), after normalization to the respective room temperature intensity (I_0) (open and full symbols refer to the heating and cooling cycles, respectively).

peak indicates a loss of the lateral correlation among the molecular segments within the smectic layers. The resulting X-ray pattern does not change substantially up to 352–355 K (Figure 2C). Above this temperature, corresponding to the second DSC endothermic transition, the small-angle peak with periodicity d_2 disappears. The spectrum is then constituted only by three small-angle peaks, the third harmonic (d = 17.4 Å) having a very low intensity, and a diffuse wide-angle halo (Figure 2B). At temperatures above 365 K (Figure 2A), corresponding to the higher temperature DSC endothermic transition, all the small-angle peaks disappear, indicating the transition to the isotropic melt. This trend of the X-ray diffraction patterns is completely reproducible in successive heating and cooling cycles. The smectic interlayer spacing d_1 is practically constant from room temperature up to the isotropization point whereas the smectic interlayer spacing d_2 regularly shortens from 34.6 Å at room temperature to 31.2 Å at 353 K. The intensities of the first-order reflection for both periodicities d_1 and d_2 (I_1 and I_2) were evaluated from the X-ray diffraction patterns after background subtraction, correction for Lorentz and polarization factors, and instrumental resolution function.[3,4] Figure 3 reports the trends of I_1 and I_2 normalized to the respective room temperature intensity (I_0) as a function of the temperature. It is apparent that the thermal evolution of the two peaks follows distinct rules. On heating, I_2 progressively decreases throughout the whole mesophasic region, whereas I_1 is nearly constant up to about 350 K and then rapidly drops to zero within a 15 K temperature range. The reverse is observed on cooling.

Additional information can be obtained from X-ray diffraction measurements on oriented specimens as attained by drawing a fiber out of the mesophase at 350 K and quenching it in liquid nitrogen. In the small-angle region there were eight Bragg spots corresponding to the first-, second-, and third-order reflections of the smectic interlayer spacing d_1 and to the first-order reflection of the smectic interlayer spacing d_2. They were aligned on the equator, thus indicating that the smectic layers, and consequently the polymer chains are parallel to the fiber axis. Diffuse crescents were detected at wide angles and in the direction perpendicular to the fiber axis which shows that the mesogenic cores are aligned along the meridian in liquidlike layers. The above diffraction pattern suggests the simultaneous presence of two disordered orthogonal smectic mesophases with monolayer (S_{A1}) and interdigitated bilayer (S_{Ad}) structures (Figure 4). Annealing the fiber for 20 h at 310 K, that is, above the glass transition temperature and below the lower temperature DSC endothermic transition, results in a substantial sharpening

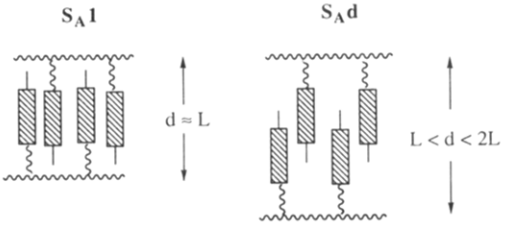

Figure 4. Schematic representation of the monolayer (S_{A1}) and interdigitated bilayer (S_{Ad}) structures of the smectic A mesophase.

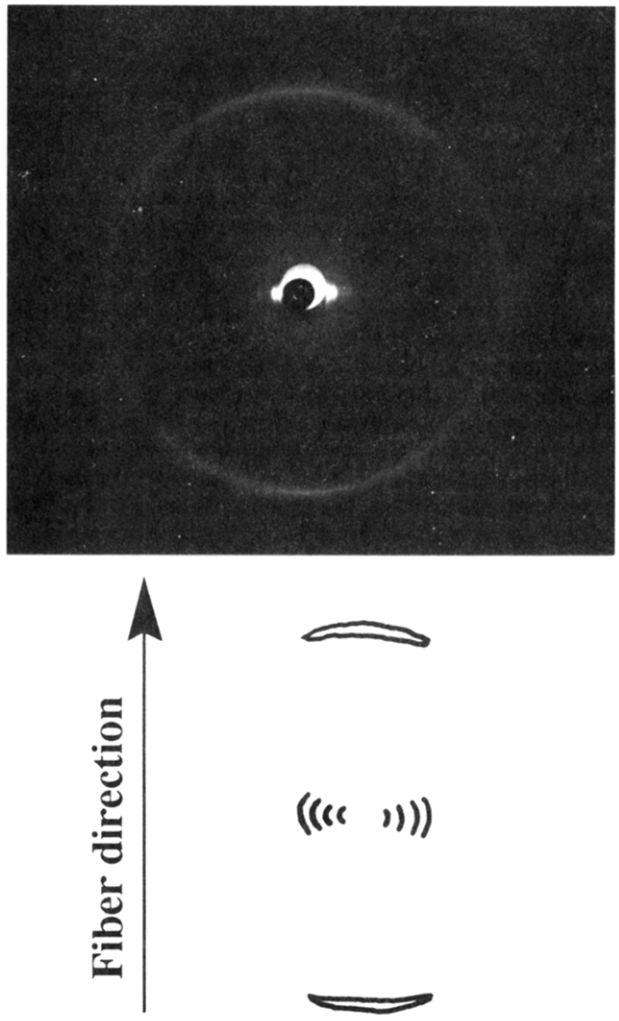

Figure 5. Fiber X-ray diffraction pattern of the smectic B mesophase of **I-8** after annealing at 310 K (vertical fiber axis) (A) and a schematic of its intensity contour map (B).

of the wide-angle crescents, thus suggesting the presence of a smectic B (S_B) mesophase with a hexagonal packing of the side chains within the smectic layers (Figure 5). However, from the width of the wide-angle peak only, it is not possible to ascertain whether the S_B mesophase originates from the transition of both S_{A1} and S_{Ad} mesophases or from either one only. Accordingly, from the above DSC and X-ray experimental results, the mesophase sequence of polymer **I-8** can be summarized as follows:

$$g \xrightarrow{299\ K} S_{B1} + S_{Bd} \xrightarrow{314\ K} S_{A1} + S_{Ad} \xrightarrow{352\ K} S_{Ad} \xrightarrow{365\ K} I$$

S_{Ad} and S_{A1} mesophases coexist in the temperature range between 314 and 352 K and undergo distinct transitions. Above 352 K the more thermodynamically stable S_{Ad} phase is only formed. In addition, two S_B mesophases, or

alternatively S_B and smectic A mesophases, coexist in the temperature range between 299 and 314 K.

The coexistence of different mesophases over a wide temperature range is a rather common feature in mixtures of low molar mass liquid crystals, including the coexistence of S_{A1} and S_{Ad} phases.[5-7] In contrast, the simultaneous formation of two mesophases being at equilibrium in side-chain liquid crystalline polymers is usually restricted to a very narrow (2–5 K) biphasic region situated between two sequential phases, especially at the nematic (or smectic) to isotropic transition.[8,9] In very few cases[10-12] has the observation of the coexistence of different smectic layer periodicities, such as d_1 and d_2, been reported. It was suggested[11] that, within the smectic A phase of some of these examples, the stacking of mesogenic units and backbones in columns of short coherence length could give rise to a column spacing (d_2), which, however, was not directly related to the smectic layer structure (d_1).

In contrast, in polymer **I-8** the different thermal evolutions of the smectic layer periodicities and of the intensities of the diffraction signals, the latter being probably due to the different temperature dependences of their structure factor, and the strongly first-order character of the transition at 352 K are consistent with the coexistence of two mesophases encompassing different thermal ranges and undergoing distinct transitions up to the S_{A1}–S_{Ad} transition at 352 K. This is in qualitative agreement with other recent results on mixtures of smectic A liquid crystals.[7] The coexistence at equilibrium over a very wide temperature region, approximately 53 K, of two different mesophases reflects the multicomponent nature of the polymeric material due to the molar mass distribution.[8,9] We have found for polymers **I-*n*** that homologues with relatively short sulfide tails ($n < 8$) exhibit monolayer smectic phases, whereas homologues with longer sulfide tails ($n > 8$) form interdigitated bilayer smectic phases.[13] Therefore, polymer **I-8** ($n = 8$) seems to be unique in that it forms both monolayer and interdigitated bilayer smectic mesophases. Corresponding to this critical length of the sulfide substituent in the polymer repeat unit, the effects of the molar mass and its dispersity can be important in determining the preferential formation of either smectic phase. It is possible that certain molar masses can facilitate the incidence of the S_{A1} phase, whereas other molar masses can preferably stabilize the S_{Ad} phase. Such mesophases will coexist in samples with wide molar mass distributions over wide temperature ranges and eventually undergo distinct transitions. To assess this hypothesis, we are presently investigating several samples of **I-8** with modeled molar masses and molar mass distributions.

Acknowledgment. This work was supported from the Ministero dell'Università e della Ricerca Scientifica e Tecnologica of Italy.

References and Notes

(1) Angeloni, A. S.; Laus, M.; Caretti, D.; Chiellini, E.; Galli, G. *Makromol. Chem.* **1990**, *191*, 2787.
(2) Angeloni, A. S.; Laus, M.; Caretti, D.; Chiellini, E.; Galli, G. *Chirality* **1991**, *3*, 307.
(3) Francescangeli, O.; Yang, B.; Chiellini, E.; Galli, G.; Angeloni, A. S.; Laus, M. *Liq. Cryst.* **1993**, *14*, 981.
(4) Francescangeli, O.; Albertini, G.; Yang, B.; Angeloni, A. S.; Laus, M.; Chiellini, E.; Galli, G. *Liq. Cryst.* **1993**, *13*, 353.
(5) Hardouin, F.; Sigaud, G.; Keller, P.; Richard, H.; Tinh, N. H.; Mauzac, M.; Achard, M. F. *Liq. Cryst.* **1989**, *5*, 463.
(6) Shashidhar, R.; Ratna, B. R. *Liq. Cryst.* **1989**, *5*, 241.
(7) Kumar, S.; Patel, P. *Condens. Matter News* **1993**, *2*, 9.
(8) Galli, G.; Chiellini, E.; Laus, M.; Caretti, D.; Angeloni, A. S. *Makromol. Chem., Rapid Commun.* **1991**, *12*, 43.
(9) Laus, M.; Angeloni, A. S.; Galli, G.; Chiellini, E. *Thermochim. Acta*, in press.
(10) Freidzon, Ya. S.; Kharitonov, A. V.; Shibaev, V. P.; Plate, N. A. *Eur. Polym. J.* **1985**, 21, 211.
(11) Sutherland, H. H.; Aliadib, Z.; Gray, G. W.; Lacey, D.; Nestor, G.; Toyne, J. K. *Liq. Cryst.* **1988**, *3*, 1293.
(12) Yamaguchi, T.; Asada, T. *Liq. Cryst.* **1991**, *10*, 215.
(13) Galli, G.; Chiellini, E.; Laus, M.; Angeloni, A. S.; Francescangeli, O.; Yang, B.; Rustichelli, F. *J. Mater. Chem.*, in preparation.